

# Performance Comparison of Liquid–Liquid Extraction in Parallel Microflows

Anil B. Vir, A. S. Fabiyan, J. R. Picardo, and S. Pushpavanam\*

Department of Chemical Engineering, Indian Institute of Technology Madras (IIT, Madras), Chennai, India 600036

**ABSTRACT:** Parallel bicontinuous flows, which include stratified and core-annular flow, have applications in liquid–liquid extraction in microchannels. The flow regime has a significant impact on interphase mass transfer. Either stratified flow or core-annular flow can result in better extraction, depending on the physical properties of the fluids and solute and the operating conditions. In this work, we systematically compare the extraction performance of core-annular and stratified flow. Mathematical models are developed for each flow regime and solved semianalytically. Both models are validated with experimental data from the literature. Using the models we analyze both flow regimes across the parameter space. Two basis for comparison are used: (i) specified flow rates of the two fluid streams and (ii) specified pressure gradient and holdup (volume fraction of the carrier stream). For core-annular flow, two distinct cases are analyzed based on the position of the solute bearing carrier stream: (i) the carrier stream is the core fluid and the solvent stream is the annular fluid and (ii) the carrier stream is the annular fluid. The results are explained in terms of two key factors: the interfacial area and the ratio of diffusion time to residence time in each fluid. This new understanding is coalesced into a set of guidelines for selecting the parallel flow regime which enhances extraction performance.

## 1. INTRODUCTION

Several applications of parallel microflows for liquid–liquid extraction have been investigated in recent years. In bicontinuous two phase parallel flow the two immiscible fluids flow alongside one another. Extraction studies have been carried out for two such flow regimes: stratified flow<sup>1–4</sup> and core-annular flow.<sup>5,6</sup> For most pairs of immiscible fluids, it is possible to operate in either flow regime by appropriately designing the inlet junction of the microchannel (Y-junction for stratified flow<sup>1,3,7</sup> and Cross-T junction for core-annular flow<sup>5–7</sup>). The following important question arises: which flow regime (core-annular or stratified) should be selected in order to maximize extraction performance and efficiency of the microchannel. This paper answers this question by providing the necessary theoretical foundation- including both qualitative understanding and quantitative results- for selecting between core-annular and stratified flow.

The emerging applications of microscale flows have attracted the attention of researchers in the last two decades. Such flows are characterized by low Reynolds numbers, small diffusion paths, and large interfacial areas per unit volume.<sup>4,8,9</sup> The latter two characteristics make microchannels efficient systems for carrying out separations and interfacial reactions, such as liquid–liquid extraction and phase transfer catalysis. The performance of these devices is closely linked to the hydrodynamics in the microchannel. Extensive studies have been carried out to determine flow regime maps in microchannels for gas–liquid and liquid–liquid flows. In the case of liquid–liquid two phase flows, different types of flow patterns are observed, depending on the geometry of the inlet of the channel, fluid properties, and flow rates. Stratified flow, core-annular flow, slug flow, and droplet flow are four commonly observed flow regimes.<sup>7,10,11</sup> At the onset of hydrodynamic instabilities, transitory flow patterns such as wavy stratified flow and wavy core-annular flow are also observed.<sup>7</sup>

Extraction studies have been carried out in segmented flows—slug and droplet flow—as well as in parallel bicontinuous flows—stratified and core-annular.<sup>1–3,5,7</sup> An advantage of parallel flows is easy separation of the phases at the end of channel.<sup>7</sup> Parallel flows are particularly relevant to separation of biomolecules in aqueous two-phase systems (ATPS).<sup>6,12–15</sup> ATPS involves only aqueous phases, which do not harm biomolecules as organic solvent do. Here segmented slug flow does not form easily, unlike conventional oil–water systems, due to weak interfacial tension effects. Instead parallel stratified or core-annular flow persists over a large range of flow rates. Thus, ATPS extraction systems are commonly operated in either stratified flow or core-annular flow.

In parallel flows, mass transfer between the carrier and solvent streams, across the fluid–fluid interface, occurs mainly by transverse molecular diffusion. The phase holdup plays a key role in determining mass transfer behavior. The phase holdup is the fraction of the volume of the channel occupied by each phase. In parallel flows, it determines the diffusion path length within each fluid. The holdup also determines the interfacial area for mass transfer in core-annular flow. Vir et al.<sup>16</sup> have studied the dependence of phase holdup on the flow rates and viscosities of the two phases in stratified and core-annular flows.

Liquid–Liquid extraction in microchannel has been applied to separate a range of solutes, including chemicals,<sup>5,17</sup> biomolecules,<sup>6,18</sup> and uranium compounds.<sup>19</sup> Novak et al.<sup>1</sup> have experimentally and theoretically analyzed extraction in ATPS. They developed a 3-D model for stratified flow to validate their experimental results. Okubo et al.<sup>2</sup> compared the

Received: December 10, 2013

Revised: April 11, 2014

Accepted: April 15, 2014

Published: April 15, 2014



extraction performance under stratified and slug flow regimes and developed a 2-D model for stratified flow. Plazl and Plazl<sup>18</sup> and Fries et al.<sup>3</sup> have analyzed liquid–liquid extraction using stratified flow both theoretically and experimentally. Malengier and Pushpavanam<sup>9</sup> compared the extraction performance of co-current and counter-current stratified flows, theoretically. Picardo and Pushpavanam<sup>20</sup> obtained conditions on the system parameters for which counter-current flow is significantly better than co-current flow. Jovanovic et al.<sup>5</sup> experimentally studied extraction in a microchannel with different types of flow patterns such as stratified, annular, slug and droplet flows. Huang et al.<sup>6</sup> recently reported the extraction of bovine serum albumin (BSA) using an aqueous two phase system (ATPS) in core-annular flow in a coaxial microchannel.

From the literature on hydrodynamics and extraction in parallel flows, it is clear that a microchannel extraction system may be operated in either stratified flow or core-annular flow. In this work, we provide a basis for selecting between the flow regimes, based on extraction performance. We take advantage of the available experimental results to develop and validate mathematical models of the extraction process in both flows, and use them to compare the two flow regimes. Several novel insights emerge from the analysis: (i) In most cases, we find that there is a considerable difference in the extraction performance of the two flow regimes. Thus, it is important to select the better flow regime for each application. (ii) We show that either core-annular flow or stratified flow may perform better, depending on the fluid properties and operating conditions. (iii) New theoretical ideas are presented for understanding and predicting the relative performance of these systems. These include the calculation of a critical core fluid holdup, which helps to identify the flow regime with a higher interfacial area for mass transfer. The diffusion time scales of the solute in each fluid is also shown to play an important role. Finally, the quantitative and qualitative results of the models are coalesced into a set of guiding principles for selecting between core-annular and stratified flow. This paper will help to select between the two flow regimes, with a minimum amount of calculation and experimentation, at an early stage of the design process. The latter is especially important since the choice of flow regime dictates the design of the inlet junction of the microchannel, as well as the stream separation section.

The paper is organized in the following manner. Section 2 is devoted to the development of mathematical models for core-annular flow in a circular microchannel and stratified flow in two geometries: (i) in a rectangular microchannel (2-D model) and (ii) between infinite parallel plates (1-D model, which is an approximation to the former 2-D model). The velocity fields in all three cases are obtained analytically. The partial differential equations describing mass transfer are solved numerically, as described in section 3. The salient features of the velocity profiles of the two flow regimes, which influence their extraction performance, are also discussed in section 3. In section 4 we compare the predictions of our models with experimental data from the literature. In section 5 we compare the mass transfer performance of stratified and core-annular flow. Two modes of comparison are considered: (i) the flow rates of both phases are specified and (ii) the pressure drop and phase holdup are specified. These input specifications are kept the same for both core-annular and stratified flow regimes. These two cases are discussed in subsections 5.1 and 5.2, respectively. Finally in section 6 we summarize the key results

and conclude with a set of practical guidelines for selecting between stratified and core-annular flow.

## 2. MATHEMATICAL MODELING OF LIQUID–LIQUID EXTRACTION IN A MICROCHANNEL

In this section the mathematical models for liquid–liquid extraction in microchannels for fully developed core-annular flow and stratified flow are obtained. In stratified flow we have analyzed both 1-D and 2-D geometries.

**2.1. L-L Extraction in a Circular Microchannel with Core-Annular Flow.** In core-annular flow one liquid occupies the central portion forming a core, while the other liquid flows around this core as an annulus, as shown in Figure 1. Here we

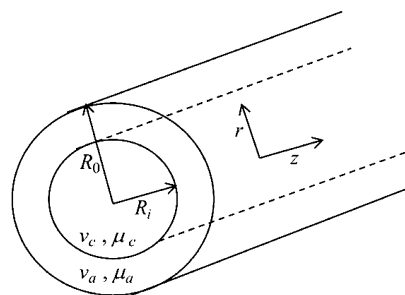


Figure 1. Schematic view of core-annular flow in a circular microchannel.

consider a circular microchannel which has a simple mathematical description. The model is also useful for core-annular flows in other geometries, as demonstrated by Vir et al.<sup>16</sup>

The Navier–Stokes equation in cylindrical coordinates is simplified under the assumption of fully developed, axisymmetric, steady laminar flow in the  $z$ -direction. Figure 1 shows a schematic view of core-annular flow in a circular microchannel. The core (annular) fluid of viscosity  $\mu_c$  ( $\mu_a$ ) flows with a velocity  $v_c$  ( $v_a$ ).

The equations are made dimensionless with the following characteristics scales

$$r_{ch} = R_0, \quad v_{c\_ch} = \frac{Q_c}{\pi R_0^2}, \quad v_{a\_ch} = \frac{Q_a}{\pi R_0^2}, \quad c_{ch} = c_{in}, \\ z_{ch} = L \quad (1)$$

The simplified dimensionless equations for velocity along with boundary conditions are

For core fluid ( $0 \leq r \leq a$ )

$$\left[ \frac{1}{r} \frac{\partial}{\partial r} \left( r \frac{\partial v_c}{\partial r} \right) \right] = G_c \quad (2)$$

For annular fluid ( $a \leq r \leq 1$ )

$$\left[ \frac{1}{r} \frac{\partial}{\partial r} \left( r \frac{\partial v_a}{\partial r} \right) \right] = G_a \quad (3)$$

The boundary conditions are

$$\text{At } r = 0, \quad v_c = \text{bounded i.e. } \frac{\partial v_c}{\partial r} = 0$$

$$\text{At } r = 1, \quad v_a = 0$$

(4)

At the interface, ( $r = a$ ), the velocity field must satisfy the following conditions:

Continuity of velocity

$$v_c = Q_r v_a \quad (5)$$

Continuity of shear stress

$$\frac{\partial v_c}{\partial r} = Q_r \mu_r \frac{\partial v_a}{\partial r} \quad (6)$$

The dimensionless parameters in the aforementioned equations are defined as

$$G_c = \frac{\pi \left( \frac{\partial p}{\partial z} \right) R_0^4}{\mu_c Q_c}, \quad G_a = \frac{\pi \left( \frac{\partial p}{\partial z} \right) R_0^4}{\mu_a Q_a}, \quad \mu_r = \frac{\mu_a}{\mu_c},$$

$$Q_r = \frac{Q_a}{Q_c}, \quad a = \frac{R_i}{R_0} \quad (7)$$

The viscosity ratio ( $\mu_r$ ) and volumetric flow rate ratio ( $Q_r$ ) are defined based on the ratio of annular phase viscosity (flow rate) to the core phase viscosity (flow rate). The holdup of a fluid is defined as the fraction of the channel's volume occupied by the fluid. The core fluid holdup is

$$\alpha_{\text{core}} = \frac{R_i^2}{R_0^2} \quad (8)$$

The annular fluid holdup is

$$\alpha_{\text{ann}} = \frac{R_0^2 - R_i^2}{R_0^2} \quad (9)$$

The holdup of the carrier phase  $\alpha_{\text{ca}}$  depends on its location. If the carrier fluid forms the core, then its holdup is given by eq 8, else, if it forms the annulus, then its holdup is determined by eq 9.

The velocity profile obtained by solving eqs 2–6 for the core and annular fluids is given by

$$v_c = \frac{G_a Q_r}{4} (a^2 - 1) + \frac{G_c}{4} (r^2 - a^2) \quad (10)$$

$$v_a = \frac{G_a}{4} (r^2 - 1) \quad (11)$$

The dimensional volumetric flow rates for both core and annular fluids are calculated by integrating eqs 10 and 11 respectively.

Next, the interphase mass transfer of the solute is modeled by the species mass balance in cylindrical coordinates. Here we assume that convection occurs only in the  $z$ -direction, while diffusion occurs only in the  $r$ -direction. Diffusion in the  $z$ -direction is neglected in comparison with convection; that is we assume that  $((v_{c,\text{ch}} L)/D_c) \gg 1$  and  $((v_{a,\text{ch}} L)/D_a) \gg 1$ . We also assume the concentration distribution to be axisymmetric, like the velocity field.

The spatial profile of dimensionless concentration for the core and annular fluids is governed by

For the core fluid ( $0 \leq r \leq a$ )

$$\frac{\partial c_c}{\partial z} = \left( \frac{1}{v_c} \right) \left( \frac{1}{Pe_c} \right) \left[ \frac{\partial^2 c_c}{\partial r^2} + \frac{1}{r} \frac{\partial c_c}{\partial r} \right] \quad (12)$$

For the annular fluid ( $a \leq r \leq 1$ )

$$\frac{\partial c_a}{\partial z} = \left( \frac{1}{v_a} \right) \left( \frac{1}{Pe_a} \right) \left[ \frac{\partial^2 c_a}{\partial r^2} + \frac{1}{r} \frac{\partial c_a}{\partial r} \right] \quad (13)$$

The dimensionless mass Peclet number for each of the fluids is based on the fluid's flow rate and the diffusivity of the solute in the respective fluid. It is the ratio of the time for diffusion across the cross-section of the channel to the residence time of the fluid (assuming the channel is completely occupied by the respective fluid).

$$Pe_c = \frac{Q_c}{\pi D_c L} \quad \text{and} \quad Pe_a = \frac{Q_a}{\pi D_a L} \quad (14)$$

Equations 12 and 13 are subject to the following boundary conditions (a) no flux at walls and (b) symmetry at the center line i.e.

$$\text{At } r = 0, \quad \frac{\partial c_c}{\partial r} = 0, \quad \text{at } r = 1, \quad \frac{\partial c_a}{\partial r} = 0 \quad (15)$$

At the interface, the concentration in the core and annular fluid are assumed to be in equilibrium with a distribution coefficient  $k_{ca}$ . The fluxes of solute must also be equal. These conditions yield:

$$\text{At } r = a, \quad c_c = k_{ca} c_a \quad \text{and} \quad -\frac{\partial c_c}{\partial r} = -D_r \frac{\partial c_a}{\partial r} \quad (16)$$

Here  $D_r$  is the diffusivity ratio and is defined as the ratio of diffusion coefficients of the annular fluid to the core fluid.

$$D_r = \frac{D_a}{D_c} \quad (17)$$

The condition at the inlet depends on whether the carrier phase is fed as the core or annular fluid

When the carrier fluid forms the core:

$$c_c^{\text{in}} = 1 \quad \text{and} \quad c_a^{\text{in}} = 0 \text{ at } z = 0$$

When the carrier fluid forms the annulus:

$$c_a^{\text{in}} = 1 \quad \text{and} \quad c_c^{\text{in}} = 0 \text{ at } z = 0 \quad (18)$$

To simulate the model, one must specify  $G_c$ ,  $G_a$ ,  $\mu_r$ ,  $\alpha_{\text{ca}}$ ,  $Pe_c$ ,  $Pe_a$ .

**2.2. L-L Extraction in a Rectangular Microchannel with Stratified Flow [2-D Model].** The stratified flow model for L-L extraction in a microchannel, with a rectangular cross-section of width  $H$  and depth  $d$ , consists of two fluids flowing parallel to each other, as shown in Figure 2. Without loss of generality, we take fluid 1 to be the carrier phase and fluid 2 to be the solvent. The Navier–Stokes equation is simplified under the assumptions of fully developed, laminar flow in the  $x$ -direction. The interface is assumed to be flat and located at a distance of  $\alpha_s$  in the  $y$ -direction (Figure 2).

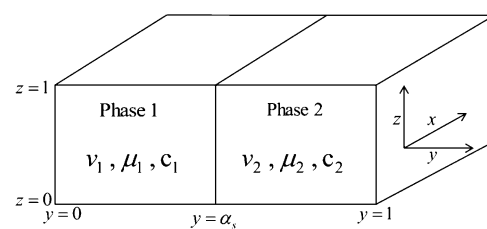


**Figure 2.** Schematic of stratified flow in a finite geometry rectangular microchannel (2-D model).

The simplified Navier–Stokes equation is made dimensionless using the following characteristic scales.

$$\begin{aligned}x_{\text{ch}} &= L, \quad y_{\text{ch}} = H, \quad z_{\text{ch}} = d, \quad v_{1\text{-ch}} = \frac{Q_1}{H^2}, \\v_{2\text{-ch}} &= \frac{Q_2}{H^2}\end{aligned}\quad (19)$$

The aspect ratio ( $\lambda$ ) is defined as the ratio of the width ( $H$ ) to the depth ( $d$ ) of the microchannel. The volumetric flow rate ratio ( $Q_r$ ) is defined as the ratio of the volumetric flow rate of the solvent phase (phase-2) to that of the carrier phase (phase-1). The holdup of the carrier phase ( $\alpha_s$ ) is defined as the ratio of interface location ( $h$ ) to the width ( $H$ ) of the channel. The dimensionless parameters are defined as

$$\begin{aligned}G_1 &= \frac{\left(\frac{\partial p}{\partial x}\right)H^4}{Q_1\mu_1}, \quad G_2 = \frac{\left(\frac{\partial p}{\partial x}\right)H^4}{Q_2\mu_2}, \quad \lambda = \frac{H}{d}, \\&\mu_r = \frac{\mu_2}{\mu_1}, \quad Q_r = \frac{Q_2}{Q_1}, \quad \alpha_s = \frac{h}{H}\end{aligned}\quad (20)$$

This results in the following dimensionless equations, which govern the velocity field:

for  $0 \leq y \leq \alpha_s$  and  $0 \leq z \leq 1$

$$\frac{\partial^2 v_1}{\partial y^2} + \lambda^2 \frac{\partial^2 v_1}{\partial z^2} = G_1 \quad (21)$$

for  $\alpha_s \leq y \leq 1$  and  $0 \leq z \leq 1$

$$\frac{\partial^2 v_2}{\partial y^2} + \lambda^2 \frac{\partial^2 v_2}{\partial z^2} = G_2 \quad (22)$$

These equations are subject to the following boundary conditions:

No slip at channel walls.

For  $0 \leq z \leq 1$  at  $y = 0$ ,  $v_1 = 0$  and at  $y = 1$ ,  $v_2 = 0$

For  $0 \leq y \leq \alpha_s$ ,  $v_1 = 0$  at  $z = 0$ ,  $z = 1$

For  $\alpha_s \leq y \leq 1$ ,  $v_2 = 0$  at  $z = 0$ ,  $z = 1$

(23)

At the interface ( $y = \alpha_s$ ), we impose

Continuity of velocity

$$v_1 = Q_r v_2 \quad (24)$$

Continuity of shear stress

$$\frac{\partial v_1}{\partial y} = Q_r \mu_r \frac{\partial v_2}{\partial y} \quad (25)$$

The 2-D velocity profile is obtained using the method of partial eigen function expansion, as described in Malengier and Pushpavanam.<sup>9,21</sup> The general solution is given by

For phase-1

$$\begin{aligned}v_1(y, z) &= \sum_{n=1}^{\infty} \left[ \frac{2G_1[(-1)^n - 1]}{n^3 \pi^3 \lambda^2} \right] [A_{1n} \cosh(n\pi\lambda y) \\&\quad + A_{2n} \sinh(n\pi\lambda y) + 1] \sin(n\pi z)\end{aligned}\quad (26)$$

For phase-2

$$\begin{aligned}v_2(y, z) &= \sum_{n=1}^{\infty} \left[ \frac{2G_2[(-1)^n - 1]}{n^3 \pi^3 \lambda^2} \right] [A_{3n} \cosh(n\pi\lambda y) \\&\quad + A_{4n} \sinh(n\pi\lambda y) + 1] \sin(n\pi z)\end{aligned}\quad (27)$$

The constants  $A_{1n}$ ,  $A_{2n}$ ,  $A_{3n}$ ,  $A_{4n}$  are obtained using the boundary conditions in the  $y$ -direction.

In this work, the first 10 terms of the series expansion are used in computations. These are found to be sufficient to ensure a converged solution to within 1% accuracy.

The dimensionless mass Peclet numbers defined for 2-D stratified flow are

$$Pe_1^{2D} = \frac{Q_1}{D_1 L} \quad \text{and} \quad Pe_2^{2D} = \frac{Q_2}{D_2 L} \quad (28)$$

The simplified dimensionless equations for stratified flow are  
For phase-1 ( $0 \leq y \leq \alpha_s$  and  $0 \leq z \leq 1$ )

$$\frac{\partial c_1}{\partial x} = \left( \frac{1}{v_1} \right) \left( \frac{1}{Pe_1^{2D}} \right) \left[ \frac{\partial^2 c_1}{\partial y^2} + \lambda^2 \frac{\partial^2 c_1}{\partial z^2} \right] \quad (29)$$

For phase-2

$$\frac{\partial c_2}{\partial x} = \left( \frac{1}{v_2} \right) \left( \frac{1}{Pe_2^{2D}} \right) \left[ \frac{\partial^2 c_2}{\partial y^2} + \lambda^2 \frac{\partial^2 c_2}{\partial z^2} \right] \quad \text{for } \alpha_s \leq y \leq 1 \\ \text{and } 0 \leq z \leq 1 \quad (30)$$

The eqs 29 and 30 are subject to the following boundary conditions.

At channel walls-

For  $0 \leq z \leq 1$

$$\text{At } y = 0, \frac{\partial c_1}{\partial y} = 0 \text{ and at } y = 1, \frac{\partial c_2}{\partial y} = 0$$

For  $0 \leq y \leq \alpha_s$

$$\text{At } z = 0, \frac{\partial c_1}{\partial z} = 0 \text{ and at } z = 1, \frac{\partial c_1}{\partial z} = 0$$

For  $\alpha_s \leq y \leq 1$

$$\text{At } z = 0, \frac{\partial c_2}{\partial z} = 0 \text{ and at } z = 1, \frac{\partial c_2}{\partial z} = 0 \quad (31)$$

at the interface ( $y = \alpha_s$ ) we have

$$\text{At } y = \alpha_s, \text{ and } 0 \leq z \leq 1 : c_1 = k_s c_2$$

$$\text{At } y = \alpha_s, \text{ and } 0 \leq z \leq 1 : -\frac{\partial c_1}{\partial y} = -D_r \frac{\partial c_2}{\partial y} \quad (32)$$

Since phase-1 is the carrier phase, we have the following initial conditions:

$$\text{At } x = 0, c_1^{\text{in}} = 1 \text{ and } c_2^{\text{in}} = 0 \quad (33)$$

**2.3. L-L Extraction in Stratified Flow between Two Infinite Parallel Plates [1-D Model].** In this section we describe a simple 1-D model of liquid–liquid extraction in the stratified flow regime. This retains the essential physics but allows easier calculations and is computationally fast. The 2-D model for stratified flow, developed in the previous section, can be directly used for flow between two infinite parallel plates (1-D model, Figure 3) by taking the limiting case of  $\lambda = 0$  in eqs 21 and 22.

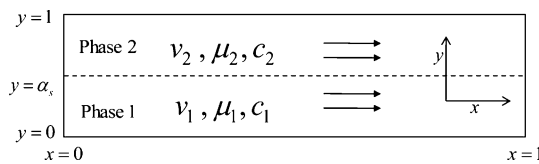


**Figure 3.** Schematic representation of stratified flow between two infinite parallel plates (1-D model).

The characteristic scales chosen for the 1-D model are analogous to the 2-D model. For flow between two infinite parallel plates the volumetric flow rate is defined per unit depth of the channel ( $\tilde{Q}_i = Q_i/d$ ). This leads to the following characteristic scales

$$y_{ch} = H, \quad v_{1\_ch} = \frac{\tilde{Q}_1}{H}, \quad v_{2\_ch} = \frac{\tilde{Q}_2}{H} \quad (34)$$

and the dimensionless parameters  $G_1$  and  $G_2$

$$G_1 = \frac{\left(\frac{\partial p}{\partial x}\right)H^3}{\mu_1 \tilde{Q}_1}, \quad G_2 = \frac{\left(\frac{\partial p}{\partial x}\right)H^3}{\mu_2 \tilde{Q}_2} \quad (35)$$

The analytically obtained dimensionless velocity profile for flow between two infinite parallel plates is

For phase-1

$$v_1 = \frac{G_1 y^2}{2} + \mu_2 \left[ \frac{G_2 \tilde{Q}_r (\alpha_s^2 - 1) - G_1 \alpha_s^2}{2(\mu_1 - \alpha_s \mu_1 + \alpha_s \mu_2)} \right] y \quad (36)$$

and for phase-2

$$v_2 = \frac{G_2 y^2}{2} + \mu_1 \left[ \frac{G_1 \alpha_s^2 - G_2 (\alpha_s^2 - 1) \tilde{Q}_r}{2 \tilde{Q}_r [(\alpha_s - 1) \mu_1 - \alpha_s \mu_2]} \right] y + \left[ \frac{G_2 \alpha_s \tilde{Q}_r [(\alpha_s - 1) \mu_1 + \mu_2] - G_1 \alpha_s^2 \mu_1}{2 \tilde{Q}_r [(\alpha_s - 1) \mu_1 - \alpha_s \mu_2]} \right] \quad (37)$$

The dimensionless mass Peclet number is defined as

$$Pe_1^{1D} = \frac{\tilde{Q}_1}{D_1} \text{ and } Pe_2^{1D} = \frac{\tilde{Q}_2}{D_2} \quad (38)$$

The dimensionless species balance for stratified flow between two infinite parallel plates is given by

For phase-1 ( $0 \leq y \leq \alpha_s$ )

$$\frac{\partial c_1}{\partial x} = \left( \frac{1}{v_1} \right) \left( \frac{L}{Pe_1^{1D} H} \right) \frac{\partial^2 c_1}{\partial y^2} \quad (39)$$

For phase-2 ( $\alpha_s \leq y \leq 1$ )

$$\frac{\partial c_2}{\partial x} = \left( \frac{1}{v_2} \right) \left( \frac{L}{Pe_2^{1D} H} \right) \frac{\partial^2 c_2}{\partial y^2} \quad (40)$$

Equations 39 and 40 are subject to the relevant subset of boundary and initial conditions given by eqs 31–33.

### 3. SOLUTION APPROACH

This section describes the methodology adopted to solve the mass transfer equations in section 2. Using the analytical expressions for the velocity profile, the partial differential equations governing the concentration of the solute are solved numerically by the method of lines (MOL). The concentration

equations are discretized in the directions perpendicular to the flow. For stratified 1-D flow and core-annular flow, only one spatial direction is discretized; whereas, the equations of the 2-D stratified model are discretized in two directions. The resulting sets of coupled ordinary differential equations are solved along the flow direction, using ode45—the explicit Runge–Kutta based solver—in MATLAB 20011a. 200 grid points are used in the radial direction for both the core and annular fluids. For the 1-D model, 200 grids are chosen in the  $y$ -direction while for the stratified 2-D model a  $30 \times 30$  grid is used in the  $y$  and  $z$ -direction in each fluid. The discretization of the flow direction is handled by the ode45 solver.

The important features of the velocity profiles obtained for the two different flow regimes are described below. The velocity profile in two phase parallel flows depends on the viscosities of the fluids and their flow rates. There is an important difference in the profiles of core-annular and stratified flow. In the case of core-annular flow, the resistance to flow experienced by the core fluid is less than the annular fluid, as the core is not in contact with the wall. Thus, the core fluid always contains the maximum of the velocity profile and flows with a higher average velocity than the annular fluid, irrespective of the viscosities of the two fluids. In the case of stratified flow, the less viscous fluid always contains the maximum axial velocity and flows faster than the more viscous fluid. Figure 4 depicts a typical dimensionless velocity profile for core-annular flow [Figure 4a] and stratified flow [Figure 4b].

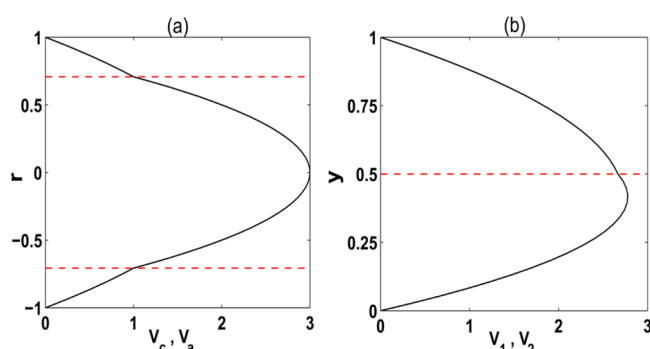


**Figure 4.** Dimensionless velocity profile of two phase parallel flows in microchannel (a) core-annular flow and (b) stratified flow between two infinite plates (1-D model). [ $\mu_r = 2$ ,  $Q_r = 0.25$  for core-annular flow model,  $Q_r = 0.833$  for stratified 1-D model,  $G_1 = -32$ ,  $G_2 = -19.2$ ,  $G_c = -5.09$ ,  $G_a = -10.18$ ,  $\alpha_s = \alpha_{ca} = 0.5$ .]

The variation of the holdup of the fluids with the flow rate fraction and viscosity ratio is very different for these two flow regimes. These relationships are discussed in detail by Vir et al.<sup>16</sup> These differences in the two velocity fields are expected to play an important role in the relative extraction performance of stratified and core-annular flow.

### 4. VALIDATION OF MODELS WITH EXPERIMENTS

In this section, the mathematical models developed in Section 2 are validated with experiments reported in the literature. The models and experiments are compared using different extraction performance indices. These are also used for analysis of our simulation results. Novak et al.<sup>1</sup> report the variation of the extraction ratio (ER) with the residence time of the solvent (phase 2). The extraction ratio is defined as the fraction of

solute in the carrier phase that is removed by the solvent stream.<sup>1,2,4,20</sup> Assuming  $c_2^{\text{in}} = 0$  we have

$$\text{ER} = \frac{c_{2,\text{out}}^{\text{avg}} Q_2}{c_{1,\text{in}} Q_1} \quad (41)$$

Here,  $c_{2,\text{out}}^{\text{avg}}$  is the average concentration of solute in the solvent phase at the outlet. The solvent phase residence time is the residence time when the solvent phase occupies the entire channel:<sup>1</sup>

$$t_{\text{res},2} = \frac{dHL}{Q_2} \quad (42)$$

The experimental data of Fries et al.<sup>3</sup> and Jovanovic et al.<sup>5</sup> are reported in terms of the extraction efficiency ( $E$ ) and its dependence on the overall residence time. Extraction efficiency is defined as the ratio of the reduction in the average concentration in the solvent phase at the outlet to the reduction when equilibrium is achieved.<sup>3,4</sup>

$$E = \frac{c_{2,\text{out}}^{\text{avg}} - c_{2,\text{in}}^{\text{avg}}}{c_2^{\text{eq}} - c_{2,\text{in}}^{\text{avg}}} \quad (43)$$

where  $c_2^{\text{eq}}$  is the equilibrium concentration of the solute in the solvent phase. The overall residence time is defined as<sup>3,4</sup>

$$t_{\text{res}} = \frac{dHL}{Q_1 + Q_2} \quad (44)$$

Figure 5a shows the comparison of our stratified models (1-D and 2-D) with the experiments of Novak et al.,<sup>1</sup> in terms

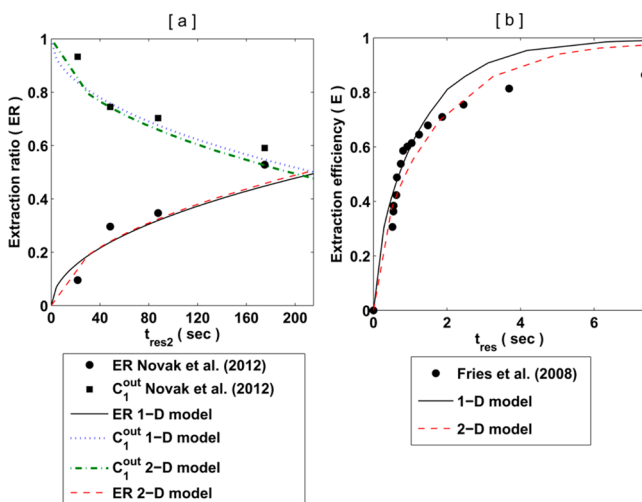


**Figure 5.** Validation of the stratified 1-D and 2-D models with experiments reported in the literature: (a) Novak et al.<sup>1</sup> [ $\lambda = 4.4$ ] (b) Fries et al.<sup>3</sup> [ $\lambda = 2.858$ ].

of the extraction ratio. In Figure 5b, the predictions of the extraction efficiency as a function of the overall residence time is compared with the data of Fries et al.<sup>3</sup> Both the 1-D and 2-D models capture the experimental behavior well. The 1-D and 2-D models are expected to agree with each other in the limit of  $\lambda \rightarrow 0$ . In Figure 5 we see that the predictions of the 1-D and 2-D models are quite similar, even for  $\lambda$  greater than unity.

Jovanovic et al.<sup>5</sup> studied the extraction of 2-butanol from toluene to water in 4 different flow regimes, including core-annular flow. In Figure 6, we compare our core-annular model's

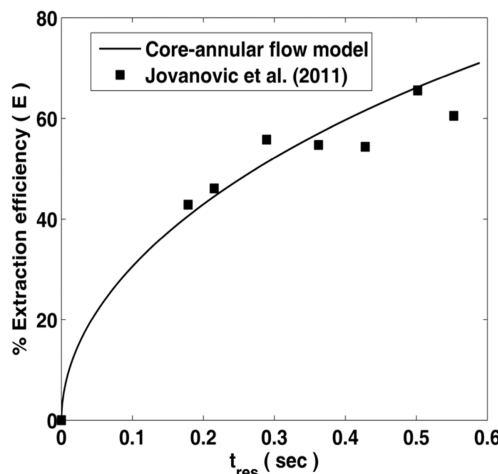


**Figure 6.** Validation of the core-annular flow model with the experiments of Jovanovic et al.<sup>5</sup>

predictions with their data of extraction efficiency as a function of the overall residence time. Here the carrier fluid is the core and the solvent fluid is the annulus. The model agrees well with the experimental data.

## 5. COMPARATIVE PERFORMANCE OF LIQUID–LIQUID EXTRACTION IN DIFFERENT GEOMETRIES

The models developed for stratified and core-annular flow are now analyzed to determine which of the systems have a better extraction efficiency or performance. The simplifying assumptions made in this work help us obtain a deeper insight into the role of the flow regime and various physical properties on extraction performance.

The comparison between channels of different geometries—rectangular for stratified flow and circular for core-annular flow—is made keeping the cross-section area the same in both cases. For a given radius of the circular channel ( $R_0$ ) and a particular aspect ratio of the rectangular channel ( $\lambda$ ), the width of the rectangular channel ( $H$ ) that has the same cross-sectional area is given by

$$H = \sqrt{\lambda} R_0 \quad (45)$$

We now define two key quantities—the ratio of characteristic times and the critical core holdup—which help us compare stratified and core-annular flow. The ratio of characteristic times ( $\tau$ ) is defined as the ratio of the diffusion time ( $t_d$ ) to the residence time ( $t_{\text{res}}$ ) of the carrier phase. The characteristic diffusion time ( $t_d$ ) is defined as the ratio of the square of the diffusion path length ( $L_d$ ) in a fluid to the diffusivity of the solute in that fluid.

$$t_d = \frac{L_d^2}{D_i} \quad (46)$$

The diffusion length of the carrier phase in stratified flow is the interface position ( $h$ ). The diffusion length scale in case of core-annular flow, when the carrier fluid flows as the core, is  $R_i$ , while it is  $(R_0 - R_i)$  when the carrier fluid flows as the annular fluid.

The residence time of the carrier phase ( $t_{\text{res}}$ ) is calculated as the ratio of the volume of the carrier phase to the carrier phase flow rate. Then the ratio of characteristic times ( $\tau$ ) is given by

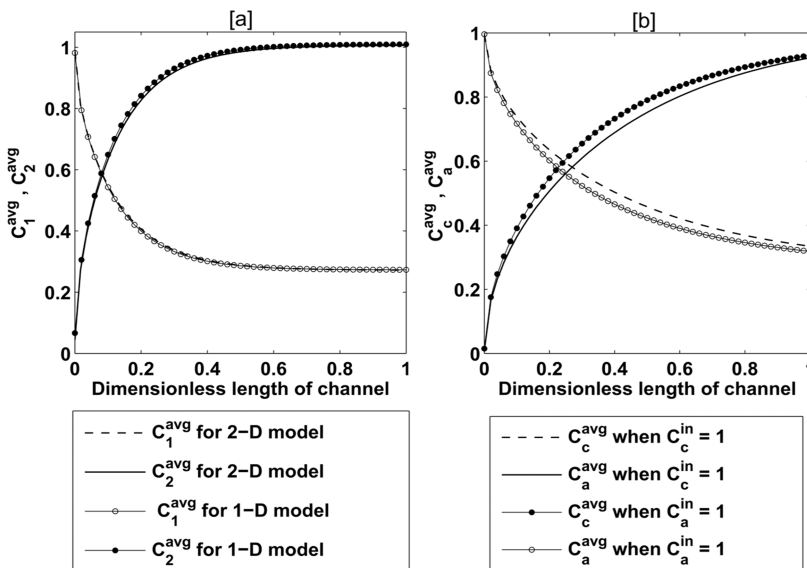


**Figure 7.** Average concentration profile of liquid–liquid extraction in a microchannel with [a] stratified flow model [b] core-annular flow model [ $k_s = k_{ca} = 0.2703$ ,  $\lambda = 0.1$ ].

**Table 1. Parameters for  $\lambda = 0.1$  of Figures 7 and 8**

model	core-annular flow when $c_c^{in} = 1$		stratified 2-D model		stratified 1-D model	
parameter	core phase	annular phase	core phase	annular phase	phase-1	phase-2
$Q_r$	0.7283		1.373		0.7283	0.7283
$\mu_r$	3		0.333		3	3
$D_r$	2.6667		0.375		2.6667	2.6667
$\alpha_i$	0.2962	0.7038	0.2652	0.7348	0.5	0.5011
$G_i$	-35.27	-16.14	-6.61	-14.45	-4.12	-38.06
$Pe_i$	2.19	4.26	4.26	2.19	6.88	114.75
$\tau$	2.193		0.719		0.345	222.85

$$\tau = \frac{t_d}{t_{res}} \quad (47)$$

The smaller the value of this ratio ( $\tau$ ), the more will be the amount of extraction that takes place. By comparing the values of ( $\tau$ ) for core-annular and stratified flow regimes, we can understand the differences in their extraction performance.

Apart from the ratio of characteristic times, the interfacial area available for mass transfer is a crucial factor in deciding the extent of extraction. The flow regime (stratified or core-annular) which has a higher interfacial area will likely result in better extraction. The interfacial area in core-annular flow depends on the holdup of the core fluid. A small core holdup, implies a small core size and lower interfacial area. On the other hand, the interfacial area in stratified flow is independent of holdup. For large core holdup, core-annular flow will have a larger interfacial area while for small core fluid holdup, stratified flow will have a larger interfacial area. The value of the core fluid holdup at which the interfacial areas in core-annular and stratified flow are equal is defined as the critical core holdup  $\alpha_{core}^{critical}$ :

$$A_{ca} = A_s \quad (48)$$

$$2\pi\sqrt{\alpha_{core}^{critical}}R_0L = L\sqrt{\frac{\pi}{\lambda}}R_0 \quad (49)$$

$$\alpha_{core}^{critical} = \frac{1}{4\pi\lambda} \quad (50)$$

When the core phase holdup is less than the critical core holdup, i.e.  $\alpha_{core} < \alpha_{core}^{critical}$ , the interfacial area in core-annular flow will be less than that in stratified flow. In such cases, stratified flow may be expected to result in better extraction.

In this section, the extraction performance of core-annular flow and stratified flow is compared in two ways: (i) Specifying the flow rates of the two phases and keeping them the same for both flow regimes. This comparison is presented in subsection 5.1. The results will help an experimentalist decide which flow regime to choose, for the required throughput of the carrier stream and the available solvent. (ii) Specifying the pressure drop and the holdup, which is kept the same for both flow regimes. This comparison is detailed in subsection 5.2. It focuses on the design of the microchannel and pumps, as well as on the operational costs associated with pumping the fluids.

**5.1. Comparison with Fixed Flow Rates.** In this section the comparison is made based on fixed flow rates of the two streams, which is kept the same in both flow regimes. The pressure gradient and the holdup are calculated iteratively from the expressions for the velocity fields in section 2.

Figure 7a compares the extraction performance in stratified flow between two infinitely long parallel plates (1-D model) with that of a microchannel with a rectangular cross-section(2-D model). The concentration, averaged over the cross-section of each fluid, is plotted along the dimensionless length of the microchannel. The parameters used to carry out the simulation are given in Table 1. The resistance of the additional walls in case of the 2-D microchannel results in a higher pressure

gradient ( $\nabla P = -1400 \text{ Pa m}^{-1}$ ) as compared to the 1-D model ( $\nabla P = -1294 \text{ Pa m}^{-1}$ ). The results show that the extraction performance for stratified flow of a rectangular microchannel can be accurately predicted with the simple 1-D model for  $\lambda = 0.1$ .

Figure 7b represents the variation of the average concentration along the dimensionless length of the channel for core-annular flow. Extraction can be carried out in two modes- with the carrier fluid as (i) the core or (ii) the annulus. Results for both cases are presented in Figure 7b. The flow rates of the carrier and the solvent streams are kept the same in both cases i.e. the flow rate of the core fluid in one case is that of the annular fluid in the other case, and vice versa. It is seen that extraction is better when the carrier fluid flows as the annular fluid.

Comparing Figure 7a,b we observe that equilibrium is reached faster in stratified flow than in core-annular flow, for the selected simulation conditions. Hence, we require a smaller length of the channel to achieve equilibrium in stratified flow. In fact, the length of the channel required to achieve equilibrium in core-annular flow was found to be approximately four times the length required for stratified flow.

Figure 8 represents the extraction performance in terms of extraction ratio for both stratified and core-annular flows. We

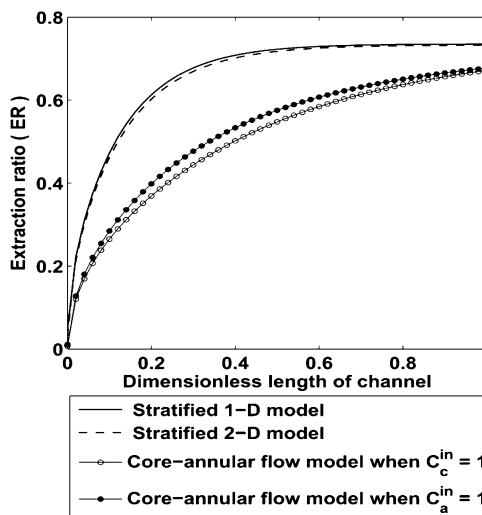


**Figure 8.** Comparison of liquid–liquid extraction performance in a microchannel based on extraction ratio (ER) for stratified and core-annular flows [ $k_s = k_{ca} = 0.2703$ ,  $\lambda = 0.1$ ].

see that the extraction performance can be predicted with good accuracy using the simpler 1-D model for stratified flow. This is to be expected, since the aspect ratio is small.

In agreement with Figure 7b, Figure 8 shows that extraction is better when the carrier stream flows in the annular region. This is because the annular fluid always flows slower than the core fluid and so has a longer residence time in the channel. This is confirmed by the lower value of the ratio of characteristic times when the carrier fluid is in the annular region, as compared to when it occupies the core ( $\tau = 0.719$  and  $\tau = 2.193$ , respectively).

Figure 8 shows that stratified flow has the best extraction performance for the selected conditions. To understand this we observe that the core phase holdup (with the carrier fluid as either the core or the annulus) is lower than the critical core phase holdup ( $\alpha_{\text{core}}^{\text{critical}} = 0.796$ ) [c.f. Table 1]. Hence the

interfacial area available for mass transfer is more in the case of stratified flow, as compared to either of the two core-annular flows. A additional reason for the superiority of stratified flow is that it has a lower value of the ratio of characteristic times ( $\tau = 0.345$ ) than either of the core-annular flows ( $\tau = 2.193$  when the carrier phase is in the core region and  $\tau = 0.719$  when the carrier phase is in the annular region). Thus, in this case, extraction takes place to a greater extent, for a given length of channel, if stratified flow is used.

Next, in Figure 9 we show a case wherein core-annular flow has a superior extraction performance. Here, we consider

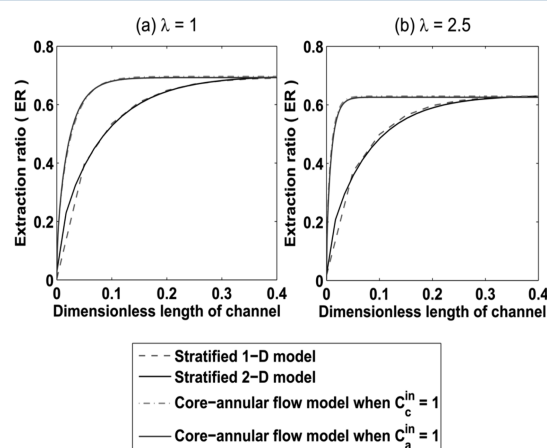


**Figure 9.** Liquid–liquid extraction performance based on extraction ratio (ER) along the dimensionless length of channel for different aspect ratios. (a)  $\lambda = 1$  (b)  $\lambda = 2.5$  [ $k_s = k_{ca} = 0.2703$ ].

stratified flow in a rectangular microchannel of two different aspect ratios  $\lambda = 1$  and  $2.5$ . Tables 2 and 3 show the dimensionless parameters used in the simulation for both cases. The performance of both types of core-annular flow is better than stratified flow, for both aspect ratios (c.f. Figure 9). In this case, the core phase holdup in both core-annular flows (carrier fluid as core or annulus) is greater than the critical core phase holdup. This is true for both aspect ratios: for  $\lambda = 1$  ( $\lambda = 2.5$ )  $\alpha_{\text{core}}^{\text{critical}} = 0.0795$  ( $\alpha_{\text{core}}^{\text{critical}} = 0.0318$ ) [c.f. Tables 2 and 3]. Hence, because of its larger interfacial area for mass transfer, core-annular flows result in better extraction than stratified flow, in Figure 9. In addition, the ratio of characteristic times is less in the case of core-annular flow (c.f. Tables 2 and 3). This further improves the relative performance of core-annular flow.

The 1-D and 2-D models are expected to match well for small aspect ratios. This is indeed the case in Figure 8. However, in Figure 9 we see that the predictions of the simpler 1-D model match well with those of the 2-D model, even for aspect ratios greater than unity. Thus, the simpler 1-D model can be used for analyzing extraction performance instead of the 2-D model, even if the aspect ratio is not very small. This will save a lot of computation time.

In this section, we have seen that there is a considerable difference in the performance of the two flow regimes. It is clear that either stratified flow or core-annular flow may be superior, depending on the physical properties and operating conditions. Importantly, we have shown that the superior flow regime can be identified, without extensive computation, based on the values of the ratio of characteristic times and the critical core holdup.

Table 2. Parameters for  $\lambda = 1$  of Figure 9a

model	core-annular flow when $c_c^{in} = 1$		core-annular flow when $c_a^{in} = 1$		stratified 2-D model		stratified 1-D model	
parameter	core phase	annular phase	core phase	annular phase	phase-1	phase-2	phase-1	phase-2
$Q_r$	0.6147		1.6268		0.6147		0.6147	
$\mu_r$	3		0.333		3		3	
$D_r$	2.6667		0.375		2.6667		2.6667	
$\alpha_i$	0.3220	0.6780	0.2226	0.7734	0.5		0.5267	
$G_i$	-32.08	-17.4	-7.25	-13.37	-80.95	-43.90	-34.89	-18.92
$Pe_i$	0.14	0.23	0.23	0.14	0.44	0.72	72.96	119.6
$\tau$	0.139		0.049		0.219		0.231	

Table 3. Parameters for  $\lambda = 2.5$  of Figure 9b

model	core-annular flow when $c_c^{in} = 1$		core-annular flow when $c_a^{in} = 1$		stratified 2-D model		stratified 1-D model	
parameter	core phase	annular phase	core phase	annular phase	phase-1	phase-2	phase-1	phase-2
$Q_r$	0.4562		2.192		0.4562		0.4562	
$\mu_r$	3		0.333		3		3	
$D_r$	2.6667		0.375		2.6667		2.6667	
$\alpha_i$	0.3687	0.6313	0.1804	0.8196	0.5		0.5703	
$G_i$	-27.46	-20.07	-8.70	-11.90	-593.83	-433.89	-31.40	-22.94
$Pe_i$	0.055	0.067	0.067	0.055	0.174	0.211	695.9	846.7
$\tau$	0.055		0.022		0.217		0.248	

## 5.2. Comparison with Fixed Pressure Gradient and Holdup.

The comparison of L-L extraction in stratified and core-annular flow regimes is now made by specifying the same pressure gradient and holdup for the two flow regimes. The flow rates corresponding to these conditions are determined from the expressions for the velocity fields in section 2.

Figure 10 shows a comparison between stratified and core-annular flow, considering two different aspect ratios, as well as

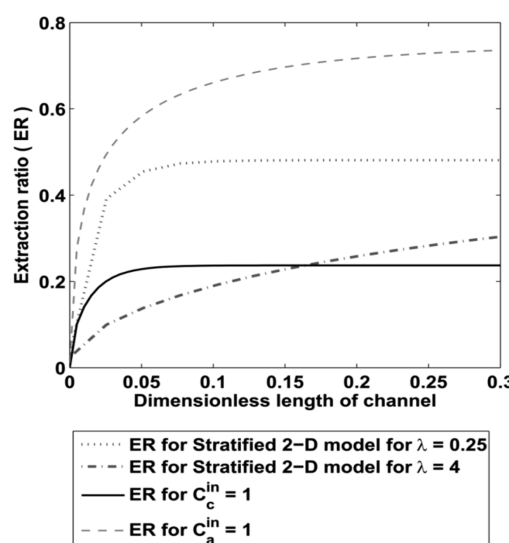


Figure 10. Liquid–liquid extraction performance at fixed pressure gradient and holdup for core-annular and stratified flow in a microchannel. [ $\alpha_s = \alpha_{ca} = 0.5$ ,  $\nabla P = -1185 \text{ Pa m}^{-1}$ ,  $k_s = k_{ca} = 0.8772$ ]

the two core-annular configurations (carrier fluid in the core or annular region). The dimensionless parameters used for the simulation are tabulated in Tables 4 and 5. Since the flow rates of the fluids in these four cases are very different, the residence times will vary considerably. Thus, the equilibrium states of these four cases show significant differences (Figure 10). Since each flow regime has different equilibrium states, they cannot

Table 4. Parameters for  $\lambda = 0.25$  of Figure 10

model	core-annular flow when $c_c^{in} = 1$		core-annular flow when $c_a^{in} = 1$		stratified 2-D model	
parameter	core phase	annular phase	core phase	annular phase	phase-1	phase-2
$Q_r$	0.2727		0.3846		0.8670	
$\mu_r$	1.6667		0.60		1.6667	
$D_r$	6.9231		0.1444		6.9231	
$G_i$	-14.55	-32.01	-7.38	-32.01	-8.80	-6.09
$Pe_i$	0.124	0.234	1.01	0.0562	0.128	0.766
$\tau$	0.124		0.010		0.016	

Table 5. Parameters for  $\lambda = 4$  of Figure 10

model	core-annular flow when $c_c^{in} = 1$		core-annular flow when $c_a^{in} = 1$		stratified 2-D model	
parameter	core phase	annular phase	core phase	annular phase	phase-1	phase-2
$Q_r$	0.2727		0.3846		0.6584	
$\mu_r$	1.6667		0.60		1.6667	
$D_r$	6.9231		0.1444		6.9231	
$G_i$	-14.55	-32.01	-7.38	-32.01	-1912.40	-1742.73
$Pe_i$	0.124	0.234	1.01	0.0562	0.1504	0.6856
$\tau$	0.124		0.010		0.301	

be compared using the ratio of characteristic times or the critical core holdup. These two quantities effect the rate of mass transfer. But if the equilibrium values are different, they do not play a significant role. Thus, although core-annular flow has a core holdup larger than critical and small characteristic time ratios, it still has a poorer performance than stratified flow. This is because the core-annular flows have lower equilibrium ER values. Thus, when the pressure drop and holdup are fixed, simulations must be carried out to determine the best flow regime and channel geometry. In the case of Figure 10, stratified flow with  $\lambda = 0.25$  has the best extraction performance. Comparing the two core-annular flows, we see that the flow with the carrier fluid in the core is better for short

channel lengths, while the flow with the carrier as the annulus is better if the channel is sufficiently long.

## 6. CONCLUSIONS

In this paper we have addressed the question of which parallel microflow regime, stratified or core-annular, should be selected for a given two phase fluid system. This choice affects the design of the microextraction system, especially the inlet junction of the microchannel and the stream separation section at the end of the channel. Thus, the choice must be made at an early stage of the design process. Ideally, the designer should be able to make this choice based on the limited information available- the fluid properties, the required throughput and the desired extent of extraction. Using the mathematical models and results presented in this paper, the flow regime can be selected which maximizes the performance and efficiency of the microchannel separator.

In summary, mathematical models have been developed for stratified and core-annular flows. The velocity profile in each case was obtained analytically and a numerical code based on the method of lines was developed to solve the mass transfer equations and predict extraction performance. These models were compared with experimental data from the literature, and showed good agreement. Importantly, we have shown that the simplified 1-D model for stratified flow predicts the extraction well, and can be used instead of the more complex 2-D model for quick calculations.

Using the models, the two flow regimes were compared considering (i) fixed flow rates of the carrier and solvent streams and (ii) fixed pressure drop and holdup of the carrier stream. The specifications were kept the same for both flow regimes. The former case focuses on the required throughputs of purified carrier stream and enriched solvent. The latter mode of comparison focuses on the pressure drop and operating costs. The results show that core-annular and stratified flow vary considerably in performance. Either of the flows can lead to better extraction, depending on the fluid properties and operating conditions. It was observed that for fixed flow rates the relative extraction performance can be described on the basis of the ratio of diffusion time to residence time ( $\tau$ ) and the interfacial area for mass transfer. The phase holdup controls the interfacial area in core-annular flow and thus plays a crucial role in deciding the superiority of core-annular flow over stratified flow. This principle was quantified by defining the critical core holdup ( $\alpha_{\text{core}}^{\text{critical}}$ ), above which core-annular flow has a higher interfacial area than stratified flow.

Two types of core-annular flows were investigated: (a) core-annular flow with the carrier fluid as the core and (b) core-annular flow with the carrier fluid as the annulus. The core fluid always flows with a higher velocity than the annular fluid and hence the residence time of the annular fluid is more. Thus, extraction is better when the carrier phase is in the annular region, than when it is in the core, provided the interfacial area is similar for both cases.

On the basis of the results presented here, we propose the following set of guidelines for selecting between stratified flow and core-annular flow for liquid–liquid extraction in a microchannel:

(i) For the given flow rates of the carrier and solvent streams, calculate the holdup of the core phase in core-annular flow for (a) core-annular flow with the carrier fluid as the core and (b) core-annular flow with the carrier fluid as the annulus. If the core phase holdup in core-annular flow (both (a) and (b)) is

less than the critical value ( $\alpha_{\text{core}}^{\text{critical}}$ ), then select stratified flow. This indicates that stratified flow will have a higher interfacial area for mass transfer. Otherwise, if one of the core-annular flow configurations has a core holdup greater than critical, it should be selected.

(ii) Among the two core-annular configurations, taking the carrier phase as the annular fluid leads to better extraction performance. Thus, if the core holdup is greater than the critical value ( $\alpha_{\text{core}}^{\text{critical}}$ ) in both (a) and (b), one should select (b), core-annular with the carrier fluid as the annulus.

(iii) Calculate the diffusion time and residence time for both core-annular and stratified flows. A low ratio of diffusion time to residence time ( $\tau$ ) favors better extraction performance. This should be considered along with the previous two guidelines.

(iv) For the specified flow rates, calculate the pressure drop in both flow regimes using the analytical results in section 2. A lower pressure drop will result in lower operational costs. The final choice should be made keeping this factor in mind, along with extraction performance.

These guidelines will help to select between stratified and core-annular flow with minimal computational and experimental effort. The correct choice of the parallel flow regime will reduce operational costs and increase the efficiency of the separation process.

## ■ AUTHOR INFORMATION

### Corresponding Author

\*E-mail: spush@iitm.ac.in. Fax+91-44-22570509.

### Notes

The authors declare no competing financial interest.

## ■ LIST OF SYMBOLS

$H$  = width of channel [m]

$d$  = depth of channel [m]

$R_0$  = radius of circular channel [m]

$\partial p / \partial z$  = constant pressure gradient in the direction of flow for core-annular flow [ $\text{Pa m}^{-1}$ ]

$\partial p / \partial x$  = constant pressure gradient in the direction of flow for stratified flow [ $\text{Pa m}^{-1}$ ]

$c_i$  = concentration of species in  $i$ th phase

$Q_i$ 's = volumetric flow rate of  $i$ th phase in stratified 2-D and core-annular flow [ $\text{m}^3 \text{s}^{-1}$ ]

$Q_r$  = ratio of volumetric flow rate of annular phase fluid (phase-2) to the core phase fluid (phase-1) in core-annular flow (2-D stratified flow)

$\tilde{Q}_i$ 's = volumetric flow rate per unit depth of  $i$ th phase in case of 1-D stratified flow [ $\text{m}^2 \text{s}^{-1}$ ]

$\tilde{Q}_r$  = ratio of volumetric flow rate per unit depth of phase-2 to the volumetric flow rate per unit depth of phase-1 fluid in 1-D stratified flow

$L$  = length of channel [m]

$D_i$  = diffusivity of  $i$ th fluid phase [ $\text{m}^2 \text{s}^{-1}$ ]

$D_r$  = ratio of diffusion coefficient of annular phase fluid (phase-2) to diffusion coefficient of core phase fluid (phase-1) in core-annular flow (2-D stratified flow)

$v_i$  = velocity of  $i$ th phase

$k_i$  = distribution coefficient of  $i$ th flow

$Pe_i$  = Peclet number of  $i$ th phase

$Pe_j^i$  = Peclet number of  $i$ th phase for  $j$ th model

$t_{\text{res}}$  = residence time [s]

$t_d$  = diffusion time [s]

**Greek Letters**

- $\alpha_{ca}$  = holdup of the carrier phase fluid in core-annular flow  
 $\alpha_s$  = holdup of carrier phase fluid in stratified flow  
 $\alpha_{core}$  = core phase holdup in core-annular flow  
 $\alpha_{ann}$  = annular phase holdup in core-annular flow  
 $\alpha_{core}^{critical}$  = critical core phase holdup in core-annular flow  
 $\lambda$  = aspect ratio ( $= H/d$ )  
 $\mu_i$  = viscosity of  $i$ th phase  
 $\mu_r$  = ratio of viscosity of annular phase fluid (phase-2) to the viscosity of core phase fluid (phase-1) in core-annular flow (stratified flow)  
 $\tau$  = ratio of characteristic times

**Subscripts**

- 1 and 2 = phase-1 and phase-2 in stratified flow  
 $a$  and  $c$  = annular fluid and core fluid in core-annular flow  
 $s$  and  $ca$  = stratified flow and core-annular flow  
1-D and 2-D = 1-dimensional and 2-dimensional stratified flow

**■ REFERENCES**

- (1) Novak, U.; Pohar, A.; Plazl, I.; Polona, Z. Ionic Liquid-Based Aqueous Two-Phase Extraction within a Microchannel System Nidaršic. *Sep. Purif. Technol.* **2012**, *97*, 172–178.
- (2) Okubo, Y.; Maki, T.; Aoki, N.; Hong Khoo, T.; Ohmukai, Y.; Mae, K. Liquid–liquid Extraction for Efficient Synthesis and Separation by Utilizing Micro Spaces. *Chem. Eng. Sci.* **2008**, *63*, 4070–4077.
- (3) Fries, D. M.; Voitl, T.; von Rohr, P. R. Liquid Extraction of Vanillin in Rectangular Microreactors. *Chem. Eng. Technol.* **2008**, *31*, 1182–1187.
- (4) Malengier, B.; Tamalapakula, J. L.; Pushpavanam, S. Comparison of Laminar and Plug Flow-Fields on Extraction Performance in Micro-Channels. *Chem. Eng. Sci.* **2012**, *83*, 2–11.
- (5) Jovanovic, J.; Rebrov, E. V.; Nijhuis, T. A. X.; Kreutzer, M. T.; Hessel, V.; Schouten, J. C. Liquid  $\text{\AA}$  Liquid Flow in a Capillary Microreactor: Hydrodynamic Flow Patterns and Extraction Performance. *Ind. Eng. Chem. Res.* **2012**, *51*, 1015–1026.
- (6) Huang, Y.; Meng, T.; Guo, T.; Li, W.; Yan, W.; Li, X.; Wang, S.; Tong, Z. Aqueous Two-Phase Extraction for Bovine Serum Albumin (BSA) with Co-Laminar Flow in a Simple Coaxial Capillary Microfluidic Device. *Microfluid. Nanofluid.* **2013**.
- (7) Kashid, M. N.; Renken, A.; Kiwi-Minsker, L. Influence of Flow Regime on Mass Transfer in Different Types of Microchannels. *Ind. Eng. Chem. Res.* **2011**, *50*, 6906–6914.
- (8) Zhao, Y.; Chen, G.; Yuan, Q. Liquid – Liquid Two-Phase Mass Transfer in the T-Junction Microchannels. *AIChE J.* **2007**, *53*, 3042–3053.
- (9) Malengier, B.; Pushpavanam, S. Comparison of Co-Current and Counter-Current Flow Fields on Extraction Performance in Micro-Channels. *Adv. Chem. Eng. Sci.* **2012**, *02*, 309–320.
- (10) Dessimoz, A.; Cavin, L.; Renken, A.; Kiwi-minsker, L. Liquid – Liquid Two-Phase Flow Patterns and Mass Transfer Characteristics in Rectangular Glass Microreactors. *Chem. Eng. Sci.* **2008**, *63*, 4035–4044.
- (11) Sarkar, P. S.; Singh, K. K.; Shenoy, K. T.; Sinha, A.; Rao, H.; G, S. K. Liquid–Liquid Two-Phase Flow Patterns in a Serpentine Microchannel.pdf. *Ind. Eng. Chem. Res.* **2012**, *51*, 5056–5066.
- (12) Hardt, S.; Hahn, T. Microfluidics with Aqueous Two-Phase Systems. *Lab Chip* **2012**, *12*, 434–442.
- (13) Tsukamoto, M.; Taira, S.; Yamamura, S.; Morita, Y.; Nagatani, N.; Takamura, Y.; Tamiya, E. Cell Separation by an Aqueous Two-Phase System in a Microfluidic Device. *Analyst* **2009**, *134*, 1994–1998.
- (14) Nam, K. H.; Chang, W. J.; Hong, H.; Lim, S. M.; Kim, D. Il.; Koo, Y. M. Continuous-Flow Fractionation of Animal Cells in Microfluidic Device Using Aqueous Two-Phase Extraction. *Biomol. Microdevices* **2005**, *7*, 189–195.
- (15) Huh, Y. S.; Jeong, C.-M.; Chang, H. N.; Lee, S. Y.; Hong, W. H.; Park, T. J. Rapid Separation of Bacteriorhodopsin Using a Laminar-Flow Extraction System in a Microfluidic Device. *Biomicrofluidics* **2010**, *4*, 14103.
- (16) Vir, A. B.; Kulkarni, S. R.; Picardo, J. R.; Sahu, A.; Pushpavanam, S. Holdup Characteristics of Two-Phase Parallel Microflows. *Microfluid. Nanofluid.* **2013**.
- (17) Sen, N.; Darekar, M.; Singh, K. K.; Mukhopadhyay, S.; Shenoy, K. T.; Ghosh, S. K. Solvent Extraction and Stripping Studies in Microchannels with TBP Nitric Acid System. *Solvent Extr. Ion Exch.* **2014**, *32*, 281–300.
- (18) Znidarsic-Plazl, P.; Plazl, I. Steroid Extraction in a Microchannel System—Mathematical Modelling and Experiments. *Lab Chip* **2007**, *7*, 883–889.
- (19) Hotokezaka, H.; Tokeshi, M.; Harada, M.; Kitamori, T.; Ikeda, Y. Development of the Innovative Nuclide Separation System for High-Level Radioactive Waste Using Microchannel Chip-Extraction Behavior of Metal Ions from Aqueous Phase to Organic Phase in Microchannel. *Prog. Nucl. Energy* **2005**, *47*, 439–447.
- (20) Picardo, J. R.; Pushpavanam, S. On the Conditional Superiority of Counter-Current over Co-Current Extraction in Microchannels. *Microfluid. Nanofluid.* **2013**, *15*, 701–713.
- (21) Malengier, B.; Pushpavanam, S.; D'haeyer, S. Optimizing Performance of Liquid–liquid Extraction in Stratified Flow in Micro-Channels. *J. Micromech. Microeng.* **2011**, *21*, 115030.